RESEARCH ARTICLE

An experimental investigation on the corrosion resistance and bond behaviour of concrete reinforced with stainless steel and carbon steel bars – a comparative study

Hanuma Kasagani[1] · Chava Srinivas[1] · K. Anjaneyula Naik[1] · S. R. R. Teja P.[1] · S. Sai Phani Swethaswari[1]

Abstract

This study aimed to investigate the corrosion rate, corrosion resistance, and bond behaviour of stainless steel (SS) bars in comparison to carbon steel (CS) bars. Concrete specimens (M30) were cast using SS (grade SS550) and CS (grade Fe550D) bars and then immersed in NaCl medium with varying concentrations (0%, 3%, and 5%). Accelerated corrosion and pull-out tests were conducted to determine the corrosion resistance and bond behaviour of the concrete, while the Natural Corrosion Rate test was performed to determine the corrosion rate. The test results revealed that CS bars failed three times faster than SS bars and exhibited a corrosion rate approximately 6 times higher than SS bars. Furthermore, the limit of corrosion initiation and propagation ratios for CS vs. SS rebar was found to be 1:1.8 weeks and 1:1.7 weeks respectively. Consequently, the bond strength of CS bars after corrosion was found to be 30% lower than that of SS bars. SEM analysis indicated that the presence of a chromium oxide film on SS steel exhibited better protective properties than that of CS steel. The chloride threshold value measured by using potentiometric titration showed that SS bars had a higher resistance against the chloride penetration approximately two times higher than that of CS bars. From this experimental study, it can be concluded that corrosion resistance, bond behaviour, protective properties and service life of SS steel bars suggest its potential superiority over CS steel bars in concrete structures.

Keywords Stainless steel (SS) · Carbon steel (CS) · Natural corrosion rate test (NCR) · Accelerated corrosion test (ACT) · Pull-out test · Bond strength · Potentiometric titration

1 Introduction

For many years, carbon steel (CS) has been the preferable option for reinforcement in concrete structures due to its high strength and ease of availability [1]. However, the corrosion of carbon steel reinforcement is one of the primary causes of deterioration of the reinforced cement concrete (RCC) structures which leads to cracking and spalling of concrete under harsh climatic conditions [2, 3]. Factors such as increased pollution levels, excessive use of de-icing salts, overloading of structures beyond their intended capacity and underestimating the impact of climatic conditions will play a

role towards the corrosion of concrete. Therefore, there is an increasing demand to enhance the durability and service life of RCC structures [4, 5]. Carbonation is one of the causes of corrosion, which destroys the protective passive layer surrounding the reinforcing bar. In marine environments, chemical and mineral processing plants, etc., the ingression of highly corrosive chloride ions through the concrete to the reinforcing bar typically causes corrosion [6, 7]. The products of corrosion, such as iron salts and oxides, will try to increase volume larger than the original steel volume, leading to the cracking and subsequent spalling of concrete [8].

Various remedial measures have been introduced to address the corrosion of reinforcement in concrete structures, such as increasing the concrete cover, using high-strength concrete, cathodic protection, reducing the water-cement ratio, applying sealants and anti-corrosion coatings such as epoxy and acrylic coatings on reinforcement bars [9–12]. The corrosion performance of mild steel and epoxy-coated rebar in concrete was evaluated under simulated

✉ S. R. R. Teja P.
raviteja.sriram@gmail.com

1   Department of Civil Engineering, Velagapudi Ramakrishna Siddhartha Engineering College, Vijayawada 521137, Andhra Pradesh, India

harsh environmental conditions by Sohail et al. [13]. The study aimed to assess the protective effectiveness of epoxy coatings in preventing corrosion and results indicated the epoxy-coated rebar demonstrated superior corrosion resistance compared to the mild steel counterpart. Epoxy-coated rebar exhibited reduced corrosion rates, minimal rust formation, and enhanced durability, showcasing its potential as an effective corrosion protection strategy in challenging concrete environments like high humidity, aggressive chemicals, and cyclic wet-dry conditions [13].

The study on the electrochemical behavior of mild and corrosion-resistant concrete reinforcing steels investigates the corrosion performance of these materials in concrete environments [14]. Factors such as corrosion rates, polarization behavior, and corrosion product characteristics are analyzed. The research explores the influence of concrete mix designs, accelerated corrosion tests, and field studies to validate laboratory findings. Additionally, the impact of stray currents, durability under thermal cycling, and performance in aggressive environments are assessed. Key findings reveal that corrosion-resistant steels exhibit superior electrochemical performance compared to mild steel [14].

However, these methods are only effective for a limited time, and they may not be suitable for harsh climatic conditions, such as high chloride-contaminated areas in addition, they may increase the dead load of structures and reduce the bond strength. Utilization of inhibitors offers a temporary solution, and using cathodic protection is challenging to implement and may require post-maintenance and monitoring [15, 16]. Replacing CS bars with low alloy steel bars up to a concentration of only 1% or so is not the solution when the concrete is exposed to high levels of urban pollution and aggressive marine environments. According to a NACE report, approximately 15% of concrete bridges, including both conventional and prestressed bridges, are structurally deficient due to corrosion, with the total direct cost of corrosion estimated at $276 billion annually. As such, the overall direct and indirect cost of corrosion exceeds 3% of the world's GDP [17].

Concrete corrosion is an electrochemical process whereby the depletion of the passivity layer around the reinforcement bar occurs and corrosion initiation takes place when the pH of concrete drops below 11 (the pH of concrete is typically 14) [6, 18, 19]. When metals with higher chromium content come into contact with oxygen, they develop a passive layer of Chromium Oxide that serves as a protective barrier against corrosion of the steel bars [20, 21]. Stainless Steel (SS) bars, which have a chromium content of at least 10.5% (generally 10.5–12%), were introduced as a replacement to CS bars as reinforcement to mitigate this issue. In contrast, the chromium content in CS is consistently less than 10.5% (generally 1.5%) [22]. SS is an alloy that consists of several components, including Chromium (providing corrosion resistance), Nickel (enhancing ductility), Molybdenum (resistance against pitting corrosion), low carbon content (facilitating weldability), and so on. There are 5 types of stainless steel, namely Austenitic, Duplex, Ferritic, Martensitic, and Precipitation hardening steel, with the first two types being commonly used for reinforcement purposes [23]. SS is not commonly used in reinforced concrete applications primarily due to its high initial cost, which is approximately 4–5 times greater than that of CS [24]. Moreover, there is limited literature available on the bonding properties of SS and concrete in comparison to the extensive research on the bond between CS and concrete.

The bond behaviour of reinforced concrete structures is the composite interaction between concrete and reinforcement bars that allows the transfer of forces and deformations between reinforcement bars and surrounding concrete [25, 26]. It consists of three parts chemical adhesion, friction, and mechanical interaction. The products formed in corrosion have a higher volume than the original steel volume and can damage the concrete cover by expansion. Because of the increased roughness at the steel bar surface during the initial stage of corrosion, the bond strength will increase [27]. Further corrosion of the reinforcing steel bar causes the concrete cover to crack, and the bond property begins to deteriorate due to the substantial reduction of the rib area, the loss of the confinement provided by the concrete cover, and the presence of lubricant corrosion products at the steel–concrete interface [28–31].

In summary, although SS is typically more corrosion-resistant than CS, its behaviour in concrete structures can be affected by a variety of factors, necessitating further research to determine its viability as a substitute for carbon steel in the design of RCC elements. It is crucial to investigate the corrosion resistance and bonding performance of both materials, both before and after corrosion, in the specific conditions and environment in which they will be utilized, to make an effective decision. The present investigation aims to study the rate of corrosion, corrosion resistance and bond behaviour of stainless-steel bars compared with CS in aggressive environment conditions. For this purpose, the specimens of concrete reinforced with SS (grade SS550) and CS (grade Fe550D) bars were exposed to varying concentrations of NaCl solution (0%, 3%, and 5%) are subjected to Normal Corrosion Rate (NCR) test, Accelerated Corrosion test (ACT) and pull-out tests respectively. The NCR of steel refers to the rate at which steel deteriorates due to environmental factors without any protective measures. Furthermore, the impact of corrosion on the bonding properties of both RCC reinforced with SS and CS bars was examined and further effect of SS and CS bars on the pre- and post-corrosion will be analysed. Scanning Electron Microscopy was used to analyze the surface morphology of the corroded

Table 1 Chemical composition and the mechanical properties of CS and SS

Grade of Steel	C	Ni	Mn	Si	P	S	Cr	N	Tensile Strength (MPa)	Elongation Percentage
CS (Fe-550 D)	0.25	–	–	–	0.04	0.04	–	–	600	16
SS (SS550)	0.03	0.06	1	1	0.04	0.03	13.5	0.05	625	17

Table 2 Chemical composition of cement

Property	Cement
Fineness	6%
Specific gravity	3.12
Density	1440 (kg/m^3)
Normal consistency	30%

bars and potentiometric titration was performed to determine the chloride threshold value.

2 Materials and methods

2.1 Materials and mix properties

SS rebars of SS 550 grade (as per IS 16651:201) [32] and CS bars of Fe-550D grade (as per IS 1786:2008) [33] were used for this study. The chemical composition and the mechanical properties of SS and CS bars are shown in Table 1. For this study, M30 grade of concrete was designed as per IS 10262:2019 [34] and the cement used along with mix proportions of the concrete were given in Table 2 and 3 respectively.

2.2 Specimen preparation

The CS and SS bars of diameters 8 mm, and 12 mm and a length of 4 cm were used (as shown in Fig. 1a and b) to conduct the NCR test. Before testing, the bars were cleaned using a 1 M H_2SO_4 solution (Fig. 1c) followed by acetone to remove any loose particles from the surface of the specimen.

Reinforced cylindrical specimens with dimensions of 100 mm×200 mm (as shown in Fig. 2) were used for both ACT and pull-out tests. Each specimen had a single reinforcing bar (either CS or SS) of diameter 12 mm, placed at the centre with a clear cover of 20 mm. The specimens were demoulded after 24 h and placed for water curing for 28 days.

Table 3 Mix proportions of the concrete

Grade of concrete	Cement Kg/m^3	Fine aggregate	Coarse aggregate	Water	SP	W/C	Mix
M30	365	683	1154	182	–	0.50	1: 1.87: 3.16

(a) SS bar specimens   (b) CS bar specimens   (c) Cleaning with 1M H_2SO_4 solution
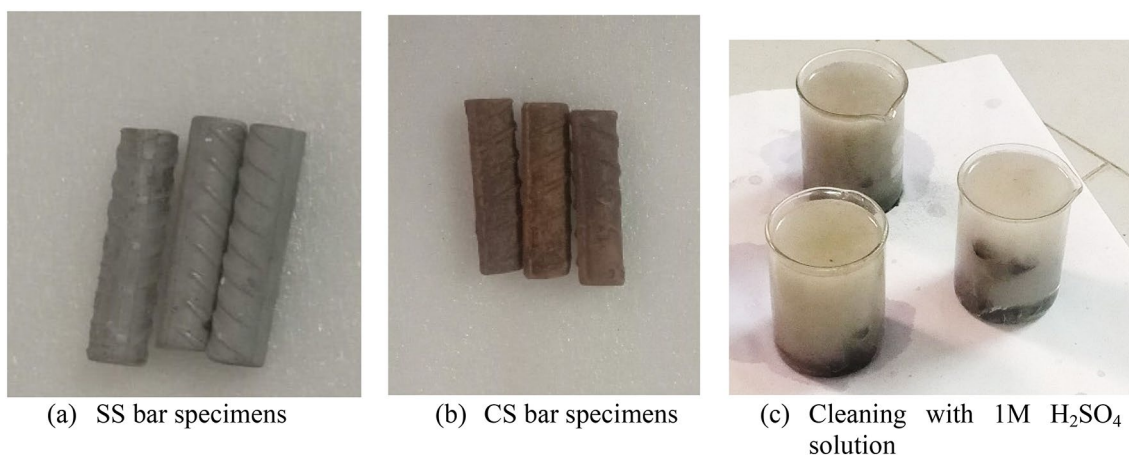
Fig. 1 Specimens for natural corrosion rate tes

Fig. 2 Cylinder specimens for ACT and pull-out test t

2.3 Test methods

2.3.1 Natural corrosion rate test

NCR test was conducted as per ASTM G31 12-a [35]. Metal weight loss is influenced by the metal's strength and the corrosive medium's reactivity. It can be viewed as a material characteristic attribute that directly affects the rate of corrosion. The CS and SS rebars of diameters 8 mm and 12 mm were immersed in NaCl solution having concentrations of 0%, 3%, and 5% at room temperature for 28, 90, 180 and 365 days (Fig. 3). The weight loss was measured by using the electrical weighing machine. Percentage weight loss of bars can be calculated by using Eq-1 and rate of corrosion can be calculated by using Eq-2.

Percentage weight loss

$$= \frac{\text{initial weight} - \text{final weight}}{\text{intial weight}} \times 100 \quad (1)$$

$$\text{Rate of corrosion} = \frac{k \times W}{D \times A \times T} \, mm/year \quad (2)$$

where k (constant) $= 87.6 * 10^4$, W $=$ Weight loss in grams, D $=$ Density of steel bar, A $=$ Surface area of bar in cm^2, T $=$ Time in hours.

2.3.2 Accelerated corrosion test (ACT)

Corrosion of concrete is an electrochemical process where the disintegration of steel occurs at the anode and the generated electrons at the anode are transferred to the cathode. This flow of electrons produces a small amount of corrosion
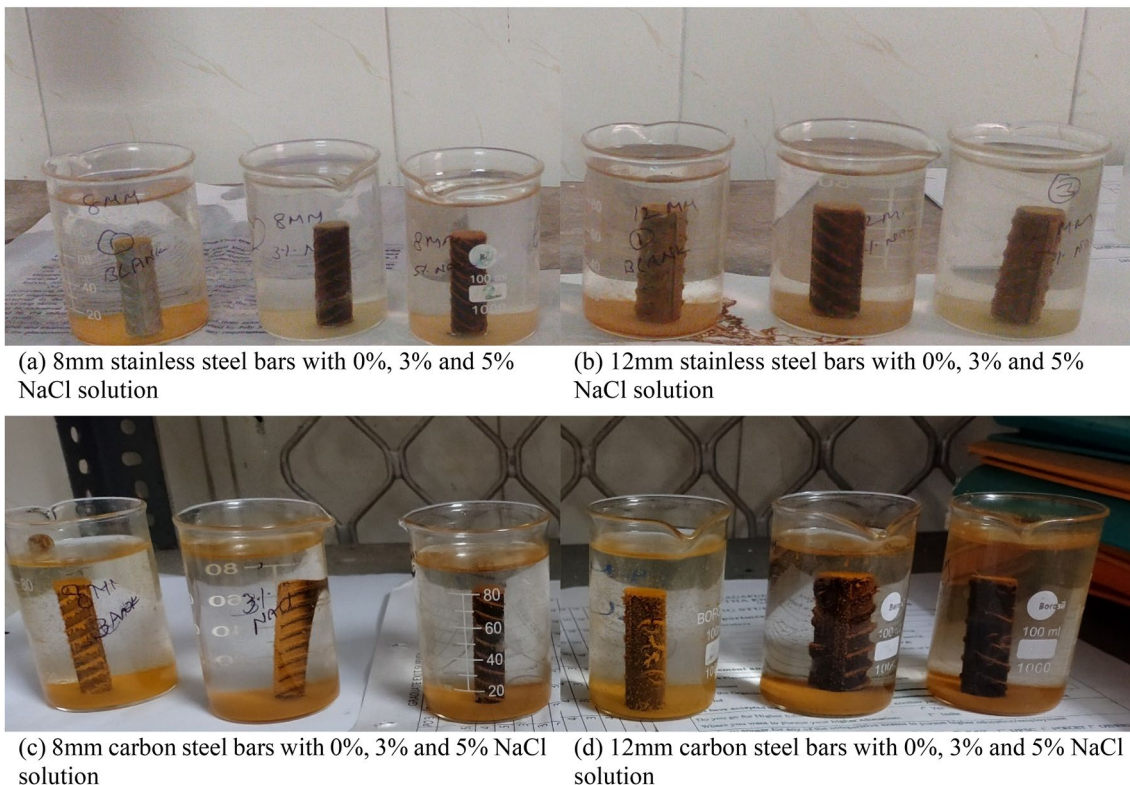
(a) 8mm stainless steel bars with 0%, 3% and 5% NaCl solution

(b) 12mm stainless steel bars with 0%, 3% and 5% NaCl solution

(c) 8mm carbon steel bars with 0%, 3% and 5% NaCl solution

(d) 12mm carbon steel bars with 0%, 3% and 5% NaCl solution

Fig. 3 Natural corrosion rate test for carbon and stainless-steel reinforcement immersed in 0, 3% and 5% NaCl solution
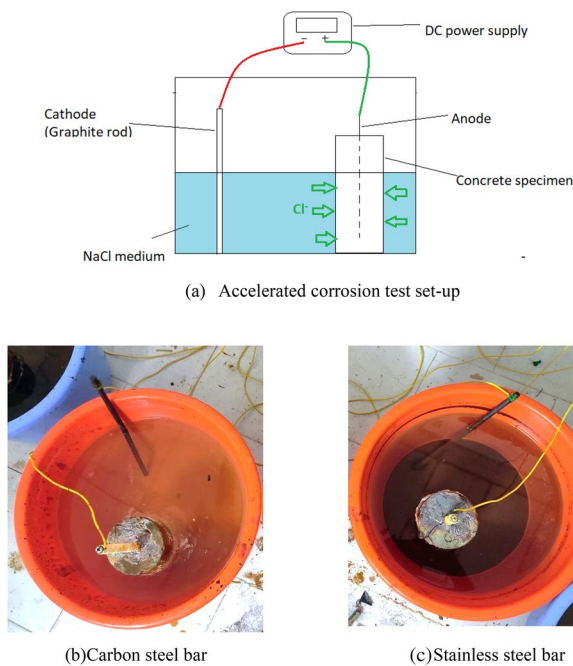
(a) Accelerated corrosion test set-up

(b)Carbon steel bar   (c)Stainless steel bar

Fig. 4 Specimens placed for accelerated corrosion test

Fig. 5 Bond test for CS and SS specimens

called corrosion current. It takes a long time to initiate the corrosion process naturally. So, for laboratory tests, the corrosion process has to be accelerated by giving an external power supply. For this, the test specimen in concrete acts as an anode, artificial graphite/calomel/stainless-steel rods are used as cathode and a salt medium (generally aqueous NaCl or CaCl$_2$) is used as an electrolyte to provide electrical contact between the anode and cathode (as shown in Fig. 4a) [36].

The test setup for conducting ACT consists of a DC power source (12 V). The test specimen (either CS or SS bar) in the concrete cylinder (working electrode) was connected to the positive terminal and a graphite rod (counter electrode) was connected to the negative terminal of the power source. The NaCl medium with varying concentrations (0%, 3%, 5%) was used as an electrolyte medium. By applying a voltage of 12 V the response of current should be noted at equal intervals of time until the first crack was observed on concrete specimen (Fig. 4b and c). The ACT test was conducted in a controlled environment (closed room) with regular monitoring, adjustments to cathodic protection systems, and the maintenance of a room temperature of 27 °C ± 3 °C to mitigate atmospheric corrosion.

2.3.3 Bond-behaviour:

The pull-out test was conducted to determine the bond strength of the specimens, which were prepared in accordance with Mohammad R. Irshidat; 2021 [37]. A Universal Testing Machine (UTM) with a capacity of 400 kN was used

for the test, and the test specimen was fixed to the UTM as illustrated in Fig. 5. Grips provided in the machine were attached to one end of the rod, which was moveable in a vertical direction. The rod was pulled upward from the specimen until it failed to achieve the maximum load. The pull-out load was applied slowly until the failure occurred, which could be either a pull-out failure or a split failure. The ultimate load, which is the maximum load at which failure occurs, was recorded in each case. The bond strength was reported as an average of three tests, and it was calculated using the equation (Eq-3).

$$\text{Bond strength}, \sigma_b = \frac{p_b}{\pi \, x \, d \, x \, l} \tag{3}$$

Where, σ_b = Bond stress (MPa), P_b = Ultimate load (kN), d = Diameter of bar (mm), L = Length of bar(m).

To investigate the bond behaviour of SS and SS embedded in concrete, a comparison was made between the bond strength before and after corrosion. The pull-out test was performed on the fresh specimens after 28 days of curing to examine the bond behaviour before corrosion. On the other hand, the specimens subjected to an accelerated corrosion test for 45 days in NaCl medium of different concentrations (0%, 3%, and 5%) were tested to assess the bond behaviour after corrosion using a pull-out test.

2.3.4 Chloride threshold value test

One of the important reasons for the corrosion of reinforcement is the ingress of chloride ions from de-icing salts

or seawater through pores. The chloride ions react chemically with the steel and the surrounding passive material to form hydrochloric acid. The hydrochloric acid eats away the steel reinforcement, causing cracking, spalling and failure of the concrete. The amount of chloride ions required at the concrete-steel interface to break the passivity layer and initiate the corrosion process is called the Chloride Threshold value (CTV).

The specimens after the accelerated corrosion test were tested for CTV since chloride content is mainly responsible for corrosion. The concrete powder was collected at the steel–concrete interface for both CS and SS specimens (Fig. 6a and b). The CTV was determined by using potentiometric titration as per IS3025 Part 32 (Fig. 6c) [38, 39]. To make the titrate 10 g of the concrete powder samples taken from CS and SS bar specimens were taken into 2 separate beakers and 100 ml of water was added into each beaker. The solutions were subjected to continuous stirring by using a Jar test apparatus at a speed of 60 rpm. After one hour of continuous stirring leave the specimen for 5 h to settle down all the suspended particles. Now 50 ml of this solution was taken into a conical flask for titration. 1 M $AgNO_3$ was taken in burette as titrant and potassium chromate was used as an indicator. When two to three drops of the indicator were added to the titrate, it turned into a yellowish green colour. The titrate was then subjected to titration by continuous

stirring. The addition of $AgNO_3$ continued until the titrate was turned into a reddish-brown colour. The strength of chloride ions was calculated by using Eqs. 4, 5 and 6.

Concentration of Chloride ions
$$= \text{Strength of chloride ions in sample} \times 1000 \, \text{ppm} \quad (4)$$

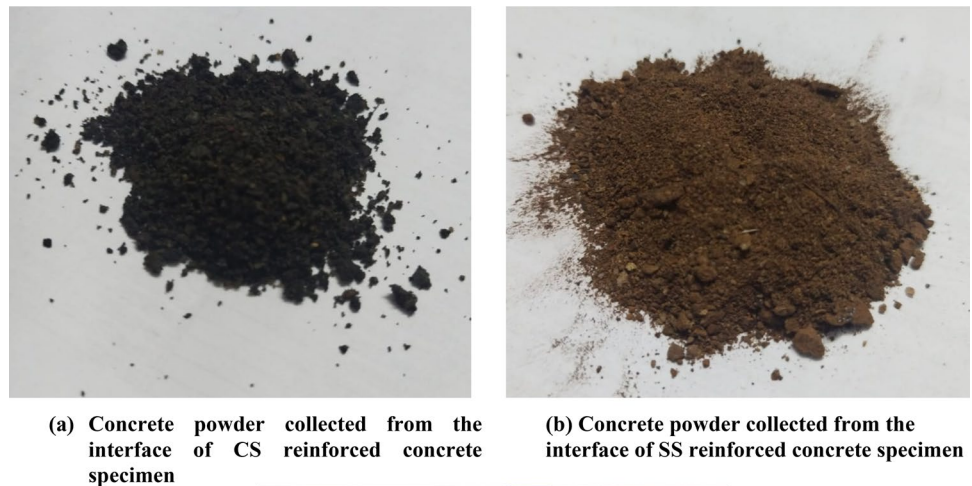where,

St, Strength of chloride ions
$$= \text{Molarity of titrate} \times \text{Molecular weight of chloride ions} \quad (5)$$

$$\text{Molarity of titrate} = \frac{\text{Molarity of AgNO3} \times \text{Volume of AgNO3 used}}{\text{volume of titrate}} \quad (6)$$

2.3.5 Surface morphology by scanning *electron* microscopy (SEM)

The samples were examined by using an Optical Microscope (OM) before SEM/EDS analysis. Olympus PMG3 optical microscope was used in this study. Using a scanning electron microscope (SEM, JEOL JSM-6400), the morphology and composition of the samples' surface were evaluated

Fig. 6 Chloride threshold value test for CS and SS

(a) Concrete powder collected from the interface of CS reinforced concrete specimen

(b) Concrete powder collected from the interface of SS reinforced concrete specimen

(c) Jar-test apparatus for making solution for titration

(Inca-sight Oxford Instruments). The samples had to have an ultrathin layer of gold on their surfaces that was applied by sputter coating. This boosted the amount of electron emissions and enhanced image capture. The secondary electrons were used to conduct SEM surface examinations. Back-scattered electron detectors were added as necessary.

3 Results and discussion

3.1 NCR test

By following the methodology given in Sect. 2.3.1 the NCR test was conducted for carbon and stainless-steel reinforcement immersing in 0, 3% and 5% NaCl solution as shown in Fig. 3. The gravimetric weight loss and percentage weight loss have been calculated for 28 days, 90 days, 180 days and 365 days and the results were shown in Fig. 7.

Based on the data presented in Fig. 7, the concentration of NaCl in the medium exhibited a positive correlation with the percentage of weight loss, regardless of the type of bar used. At 28 days, the minimum to a maximum

weight loss of SS bars and CS bars are 0.38–0.86%, and 1.29–2.76% respectively. After 90 days, the SS bars and CS bars had a minimum to a maximum weight loss of 2.48–5.45% and 9.84–14.76% respectively. Over 180 days, the SS bars and CS bars had a minimum to a maximum weight loss of 1.84–3.74% and 2.68–8.59% respectively. At the end of the 365 day study, the minimum and maximum weight losses observed were 3.21–8.99% and 10.40–24.35% for SS bars and CS bars respectively.

This means that adding more NaCl to the medium can potentially lead to a greater percentage of weight loss in both SS and CS bars. After 90 days, the SS bars had a greater weight loss percentage (9.84–14.76%) compared to CS bars (2.48–5.45%) over 180 days. However, by the end of the 365 day study, the SS bars had a smaller weight loss percentage (10.40–24.3).

The results suggest that the corrosion (weight loss) of both SS and CS bars is influenced by the concentration of NaCl in the medium. CS bars were consistently showed higher weight loss, indicating higher susceptibility to corrosion compared to SS bars. The study provides insights into the corrosion behavior of these materials over an extended
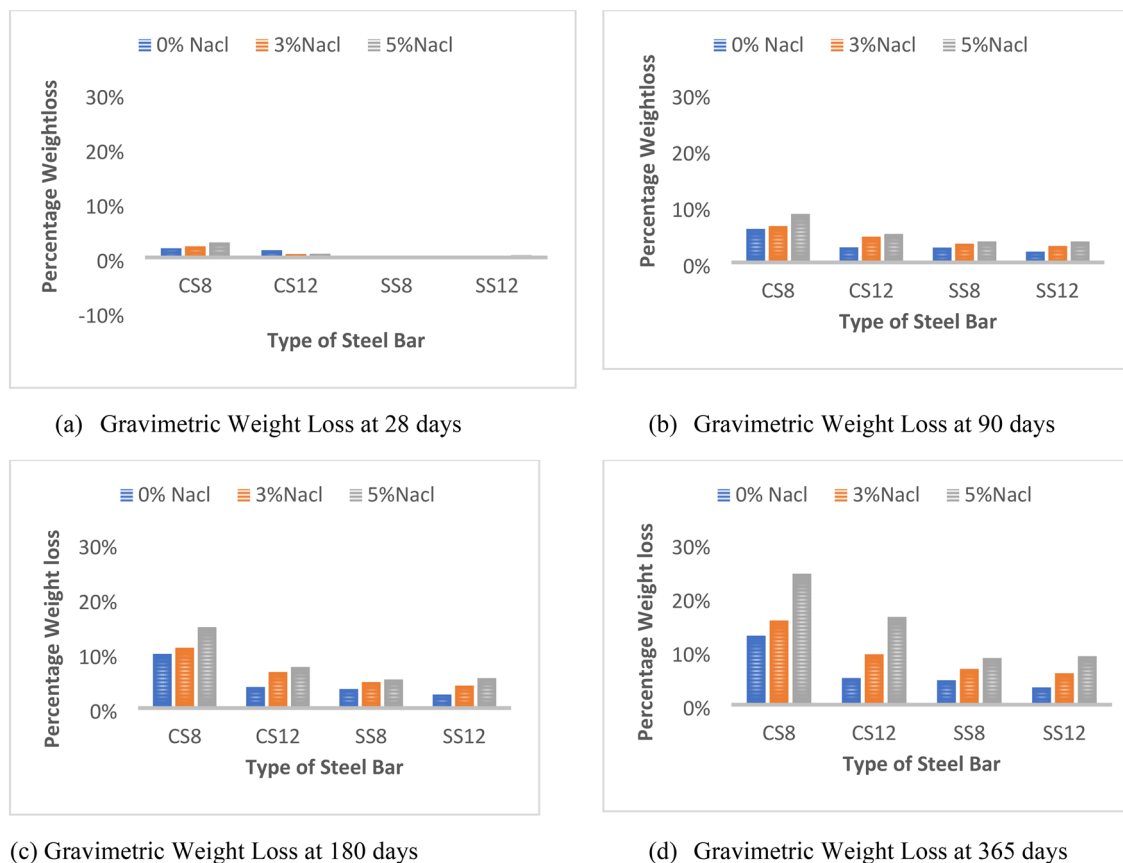

(a) Gravimetric Weight Loss at 28 days

(b) Gravimetric Weight Loss at 90 days

(c) Gravimetric Weight Loss at 180 days

(d) Gravimetric Weight Loss at 365 days

Fig. 7 The gravimetric weight loss and percentage weight loss have been calculated for 28 days, 90 days, 180 days and 365 days

period, which may have implications for their use in specific environments.

Previous research has indicated that the loss of carbon steel in comparison to SS rebars falls within the range of 5–25% [40, 41]. This loss in the tensile capacity of reinforcement may be attributed to two primary factors: (i) a decrease in the effective diameter of the reinforcement bars, and (ii) a diminished bond between concrete and steel at the reinforcement level. Typically, both factors (i) and (ii) work in tandem, potentially leading to a substantial reduction in load-bearing capacity and overall structural performance.

Furthermore, by using Eq. 2, the rate of corrosion for CS and SS bars was calculated and the same was presented in Fig. 8. After a period of (28 days, 90 days, 180 days and 365 days) the maximum rate of corrosion is noticed to be (0.106 mm/y, 0.135 mm/y, 0.24 mm/y and 0.286 mm/y) and (0.596 mm/y, 0.628 mm/y, 0.774 mm/y and 0.84 mm/y) for SS bars and CS bars respectively. Further from these results of the rate of corrosion, it can be interpreted that with an increase in the concentration of NaCl, the rate of corrosion has been increased for both SS and CS bars. However irrespective of NaCl dosage and number of days, the corrosion rate of CS bars was considerably higher than SS bars. The increment in corrosion rate is that the CS bars exhibited defects such as cracks, voids and crevices on the surfaces compared to the SS bars, and these defects were more pronounced as the concentration of NaCl increased, thereby influencing the rate of corrosion and this can be validated by observing the figures present in Fig. 9. From the findings of NCR Test, it can be concluded that the rate of corrosion of SS bars are significantly lower than the CS bars and it was found that CS bars have corroded 4–5 times than SS bars.

Similar findings were noted in prior investigations, revealing that the progression of corrosion is heightened when cracks, voids, and crevices develop on the material surface over time. CS bars displayed susceptibility to pitting attacks, specifically in the presence of elevated NaCl concentrations, manifesting as cracks, voids, and crevices on the rebars' surfaces. In contrast, SS bars exhibited remarkable resistance to both types of corrosion—pitting corrosion and uniform corrosion [42, 43].

The defects on the surfaces of CS bars, coupled with the higher corrosion rate, suggest that corrosion is likely causing structural weakening. Cracks, voids, and crevices can
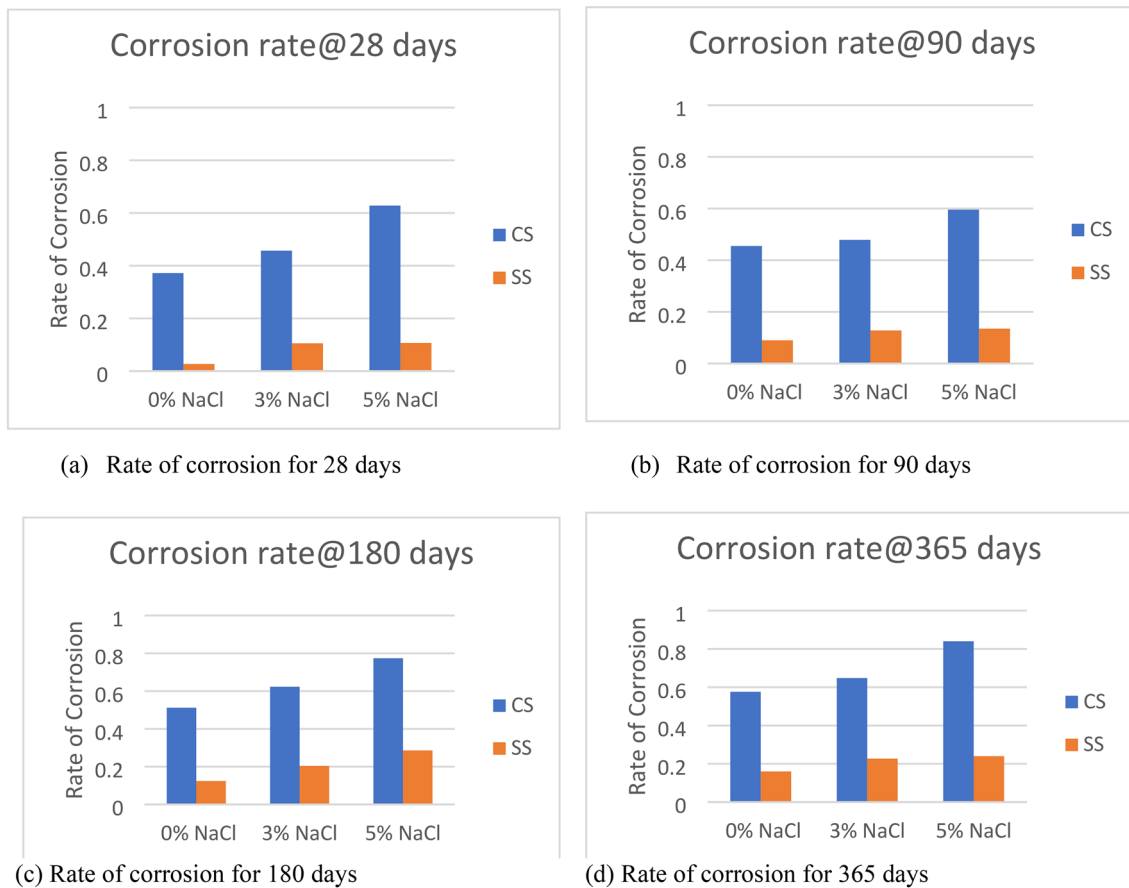

(a) Rate of corrosion for 28 days

(b) Rate of corrosion for 90 days

(c) Rate of corrosion for 180 days

(d) Rate of corrosion for 365 days

Fig. 8 Rate of corrosion calculated for 28 days, 90 days, 180 days and 365 days

(a) SS bars after 28 days of immersion

(b) CS bars after 28 days of immersion

(c) SS bars after 90 days of immersion

(d) CS bars after 28 days of immersion

(e) SS 8mm bar after 365 days of immersion in 5% NaCl medium

(f) CS 8mm bar after 365 days of immersion in 5% NaCl medium

Fig. 9 Steel specimens after immersion in NaCl solution

act as initiation sites for corrosion, and the corrosion process can exacerbate these defects, leading to a reduction in the mechanical strength of the CS bars. Hence, the SS bars exhibit fewer defects and experience a lower corrosion rate suggests that they are more resistant to corrosion-induced degradation. This resistance can contribute to better mechanical performance, making SS bars a more durable and reliable choice in corrosive environments.

3.2 ACT results

As per the procedure mentioned in Sect. 2.3.2, accelerated corrosion tests were performed on SS bars and CS bars specimens with different NaCl concentrations these results are represented in Table 4 and their variation is shown in Fig. 10. Based on the analysis of results, the damaging

process due to chloride-induced reinforcement corrosion can be categorized into two phases. The first phase is the corrosion initiation phase, during which chlorides penetrate the concrete and reach the reinforcement in sufficient quantities to depassivate the steel and initiate corrosion. The second phase is the corrosion propagation phase, where distinct levels of damage build-up were observed, including concrete cracking, spalling, and delamination of the concrete cover. These limit states, namely corrosion initiation, propagation (concrete cracking, spalling, and delamination), and ultimately structural failure, are depicted in Fig. 11 and are considered for assessing the performance of structures affected by reinforcement corrosion.

As per Table 4, In the case of CS rebar with 0% NaCl, the corrosion initiation current was found to be 43 µA from the 6th week onwards, corrosion propagation current

Table 4 Corrosion initiation and propagation periods of SS bars and CS bars

Type of bar	The concentration of NaCl medium	Initiation		Propagation		Current at failure (micro amp)
		Current (micro amp)	Period (weeks)	Current (micro amp)	Period (weeks)	
Stainless steel (SS)	0%	70	16	130	19	Upto 300
	3%	50	12	110	15	Upto 250
	5%	40	10	80	12	Upto 180
Carbon steel (CS)	0%	43	6	85	8	Upto 125
	3%	33	4	55	6	Upto 110
	5%	23	3	50	4	Upto 100

Fig. 10 Corrosion current values obtained from accelerated corrosion test

Corrosion behaviour of HYSD & SS Reabr
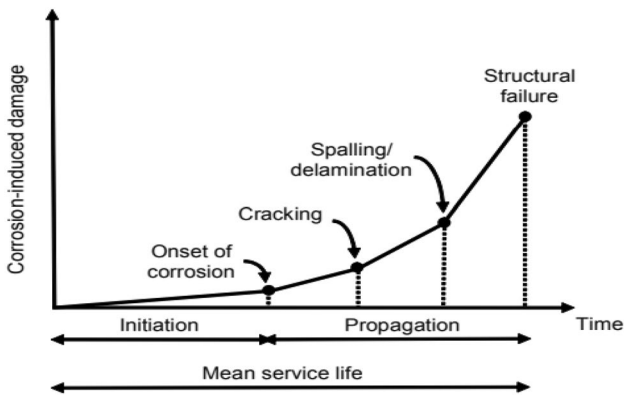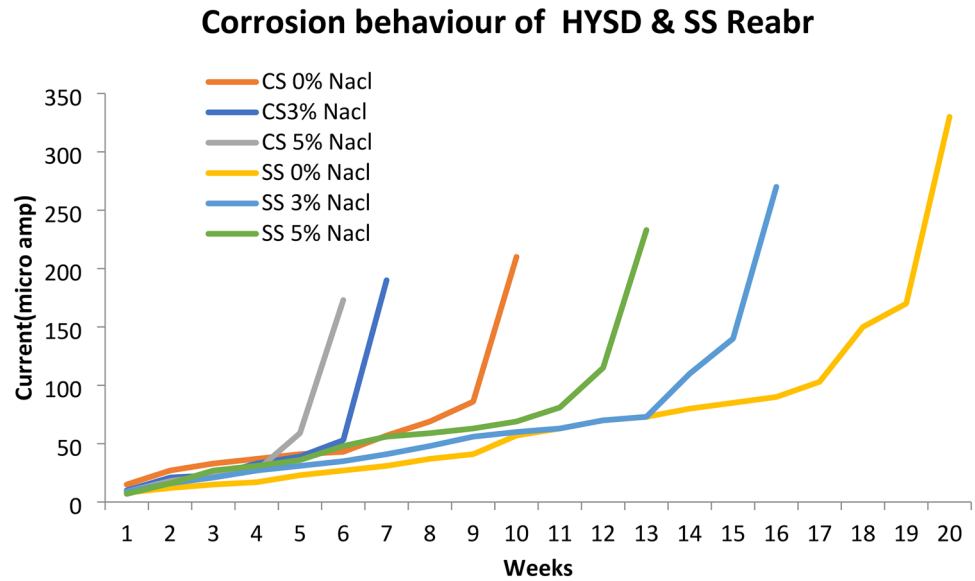
Fig. 11 Service life of stainless-steel concrete structure [39]

from the 4th week onwards, corrosion propagation current was found at 55 µA from 4th to the 6th week region. After this period, there was an abrupt increase in corrosion current from 55 µA to 110 µA. In case of CS rebar with 5% NaCl, corrosion initiation current was found at 23 µA from the 3rd week onwards, corrosion propagation current was found at 50 µA from the 3rd to 4th week region. After this period, there was an abrupt increase in corrosion current from 50 µA to 100 µA.

From Table 4, in the case of SS rebar with 0% NaCl, the corrosion initiation current was found at 70 µA from the 16th week onwards, corrosion propagation current was found at 130 µA from the 16th to 19th week region. After this period, there was an abrupt increase in corrosion current from 130 µA to 300 µA. For SS rebar with 3% NaCl, the corrosion initiation current was found at 50 µA from the 12th week onwards, and the corrosion propagation current was found at 110 µA from 12 to 15th week. After this period, there was an abrupt increase in corrosion current from 110 µA to 250 µA. In the same way for SS rebar with 5% NaCl, corrosion initiation current was found at 40 µA from the
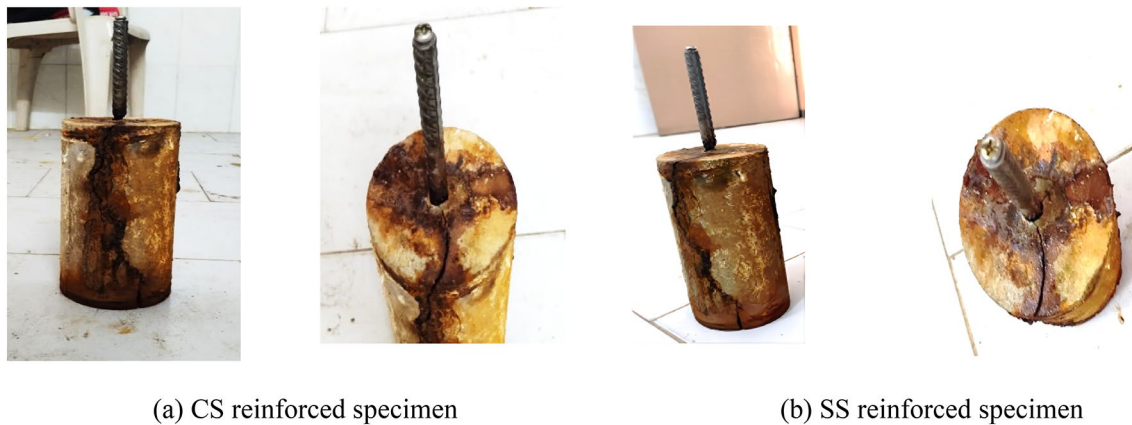
was found at 85 µA from 6th week to the 8th week region. After this period, there was an abrupt increase in corrosion current from 85 µA to 125 µA. In case of CS rebar with 3% NaCl, corrosion initiation current was found at 33 µA

(a) CS reinforced specimen   (b) SS reinforced specimen

Fig. 12 Specimens placed under accelerated corrosion test

10th week onwards, and corrosion propagation current was found at 80 µA from the 10th to 12th week region. After this period, there was an abrupt increase in corrosion current from 80 µA to 180 µA.

Microcracks were observed during the corrosion initiation phase of CS rebar specimens with 0%, 3%, and 5% NaCl concentration at 6, 4, and 3 weeks, respectively. Subsequently, major cracks were observed during the corrosion propagation phase (Fig. 12a) after 8, 6, and 4 weeks, respectively. On the other hand, SS rebar specimens indicated a longer time to failure, with corrosion initiation observed at 16, 12, and 10 weeks for specimens with 0%, 3%, and 5% NaCl concentration, respectively. Major cracks were observed during the corrosion propagation phase (Fig. 12b) after 19, 15, and 12 weeks, respectively.

The progress of corrosion initiation and propagation was found to be significantly dependent on the concentration of chlorides and the number of free chlorides. Increased supply of chlorides led to de de-passivation of anodic areas and the growth of individual corrosion pits, resulting in the formation of an extensive corrosion area. The rate of corrosion initiation and propagation was higher in CS bar specimens with increasing chloride concentration compared to SS bar specimens, as evident from Fig. 11. Furthermore, less corrosion current was observed in SS specimens compared to CS specimens until failure. This indicates that the limit of corrosion initiation and propagation ratios was observed to be 1:1.8 weeks and 1:1.7 weeks, respectively, for CS vs SS rebar. Based on this experimental study, the total service life of stainless-steel concrete structures was found to be nearly twice that of carbon steel concrete structures.

Finally, it indicates that the time of failure of CS rebar specimen with 0%, 3% and 5% NaCl concentration was 6,4 and 3 weeks and further, a major crack was observed (Fig. 12a) after 8, 6 and 4 weeks respectively. Whereas in the case of SS rebars, it indicated that the time of failure of

SS rebar specimens with 0%, 3% and 5% NaCl concentration was 16, 12 and 10 weeks and further, a major crack was observed (Fig. 12b) after 19, 15 and 12 weeks respectively. It shows that the SS rebar specimen has taken more time to fail compared to CS bars. Further, less corrosion current was observed in the protected specimen compared to CS specimen till failure.

Considering the average initiation time across these investigations, a notable reduction of approximately 70–80% is observed for CS in concrete specimens compared to the average initiation time noted for SS rebars in concrete specimens, as reported in Ref. [44] for cracks measuring 20–40 µm wide. Nevertheless, the findings of this study also imply that the impact of longitudinal micro-cracks on corrosion initiation is contingent on the crack's depth. The corrosion initiation time may experience a substantial reduction if the crack extends to the depth of the rebar.

The findings suggest that the corrosion rate of RCC members is impacted by both crack spacing and the quantity of reinforcement. While current industry practice considers corrosion initiation as the indicator for the end of service life, it is observed that corrosion initiates rapidly in cracked regions. This prompts the proposal to redefine residual structural service life, focusing on the corrosion rate during the propagation phase and establishing a limit state based on a predefined threshold loss of reinforcing steel. Furthermore, the prediction of residual service life is recommended to take into account both crack spacing and reinforcement density for a more comprehensive assessment.

3.3 Bond behaviour

A pullout test was conducted on CS and SS bars before and after corrosion as per the procedure given in 2.3.3 and the bond strength results obtained from the pull-out test were given in Table 5. The bond strength value of CS bars

Table 5 Bond strength of SS bars and CS bars before and after corrosion

Type of steel	Diameter of bar (mm)	Bond strength before corrosion (MPa)	Bond strength after corrosion	
			NaCl medium concentration	Bond strength (MPa)
Carbon steel	12	27.8	0%	18.5
			3%	10.2
			5%	5.7
Stainless steel	12	26.5	0%	25.1
			3%	22.6
			5%	20.3

without corrosion was initially measured as 27.8 MPa. However, after corrosion, it decreased significantly to 18.5 MPa in 0% NaCl medium, 10.2 MPa in 3% NaCl medium, and 5.7 MPa in 5% NaCl medium respectively. This corresponds to a nearly 5 times drop in bond strength compared to before corrosion. On the other hand, the bond strength values of SS bars were measured at 26.5 MPa before corrosion, decreased only slightly to 25.1 MPa in 0% NaCl medium, 22.6 MPa in 3% NaCl medium, and 20.3 MPa in 5% NaCl medium respectively after corrosion. This corresponds to a drop of only around 0.05 times compared to before corrosion.

Also, irrespective of the type of rebar, the bond strength decreases with an increase in the concentration of NaCl medium. Before corrosion, all the specimens were failed by concrete cover cracking and the failure was sudden with the formation of longitudinal cracks (Fig. 13a). After corrosion, due to a greater corrosion rate all the specimens having CS bars failed by pulling out of concrete whereas for SS bars due to a lesser corrosion rate, the specimen is failed by concrete cover cracking (Fig. 13b). These results demonstrated that though the bond strength of CS bars before corrosion was slightly higher than that of SS bars after corrosion the bond strength of CS bars was found to be 30% lower than that of SS bars.

Also, irrespective of the type of rebar, the bond strength decreases with an increase in the concentration of NaCl medium. Before corrosion, all the specimens were failed by concrete cover cracking and the failure was sudden with the formation of longitudinal cracks (Fig. 13a). Therefore, due to greater corrosion of CS bars all the specimens of it were failed by pulling out of concrete whereas for lower corrosion exhibited by SS bars, the specimens of it were failed by concrete cover cracking (Fig. 13b).

Interestingly, corrosion has a positive impact on the bond strength of stainless-steel specimens, which is approximately 71% higher than that of carbon steel specimens. This behavior aligns with findings from prior experimental research, as summarized in fib [45], and is consistent with observations during the post-cracking stage induced by corrosion in this experimental study.

The decline in bond stresses after the peak load, attributed to increasing corrosion, was more prominent in carbon steel specimens compared to stainless-steel specimens, ranging from 17 to 69%. Particularly, as slip increased, the bond stress of CS specimens exhibited a more pronounced reduction than that of SS specimens. This phenomenon was a result of the absence of interaction between the rebar and concrete, leading to a rapid decline in bonding.

(a) Bond failure Before Corrosion   (b) Bond failure after Corrosion

Fig. 13 Failure specimen in pull-out test

Notably, the anomalous behavior of CS specimens, displaying lower bond strength values than SS specimens at corrosion concentration levels of 0% and 5%, aligns with previous experimental results reported by Rodriguez et al. [46, 47]. Consequently, the results imply that the bond behavior is more robust in carbon steel specimens prior to corrosion, while post-corrosion, stainless steel demonstrates a more effective bond behavior compared to carbon steel specimens.

3.4 Chloride threshold value test

By conducting the chloride threshold value test, the following test results obtained from potentiometric titration are given in Table 6. After corrosion, the chloride content at the interface of concrete and CS rebar was found to be 0.063 kg/m^3 while the chloride content at the interface of concrete and SS rebar was found to be 0.103 kg/m^3. As chloride-induced corrosion is more prone in aggressive environments the bars have to show a great resistance towards chloride ions and thus should possess high CTL values. The results have shown that SS bars had chloride content about two times more than that of carbon steel bars. This means that SS bars shows great resistance towards chloride induced corrosion when compared with CS bars. These results were aligned with previous experimental results reported by Villagrán-Zaccardi et al. [48]. As per existing literature, the chloride

content for carbon steel is documented to fall within the range of 0.2–2% by the mass of cement at the interphase. In contrast, stainless steel registers a higher content of 3.5% by the mass of cement at the interphase. This difference indicates that stainless steel hinders chloride ion penetration more effectively than carbon steel, thereby enhancing its resistance to corrosion from the surrounding environment [49].

3.5 Surface morphology by scanning *electron* microscopy (SEM)

Figure 14 shows the SEM images of the surfaces of Fe550D steel and SS550 steel immersed for 180 days in the 5% NaCl solutions. Figure 14a is the SEM image of Fe550D, in which the corroded surface was observed. It shows that the surface of the CS bar was severely corroded with the formation of different forms of corrosion products (iron oxides) and was covered by a scale-like black corrosion product, over which another corrosion product was growing and appearing in the form of white clusters at several sites. Figure 14b is the SEM image of an SS550 steel specimen, where a smooth surface with a few small notches of corrosion products was observed. The corrosion product deposits observed in Fig. 14b show that the appearance of the protected surface was quite different from that of the corroded surface of the CS bar. It indicates that the penetration of chloride ions from the environment onto the substrate was effectively controlled by SS550 steel compared to Fe550D steel. From the SEM analysis, it can be inferred that the chromium (Cr) film that is present on the SS steel exhibits good protective properties for SS 550 steel over its Fe550D steel. Further, the SEM observations are confirming the results of the gravimetric studies and the accelerated corrosion studies.

Table 6 Chloride threshold values for specimens

Type of bar	Chloride threshold value (kg/m^3)
CS	0.063
SS	0.103

Fig. 14 SEM images of CS bar and SS bar after corrosion
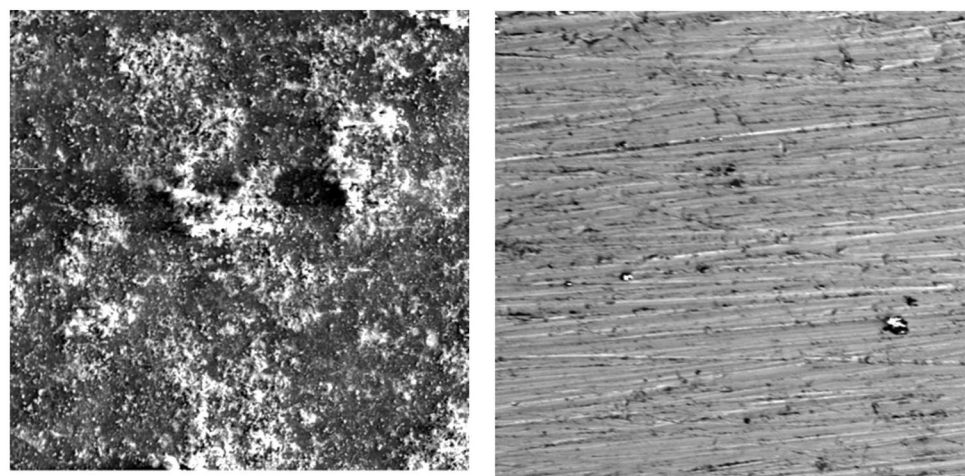
(a) CS (Fe 550D)   (b) SS (SS550)

It can be concluded that the corrosion resistance of SS bars is significantly better than that of CS bars due to the higher stability of their passive film. This film contains a high percentage of chromium and is firmly bonded to the parent metal, allowing it to self-heal in the presence of oxygen. This passive film plays a crucial role in controlling Stress Corrosion Cracking in SS concrete compared to CS concrete. similar results have been observed in studies involving carbon steel with concrete modified using carbon nanotubes, as well as stainless steel in traditional concrete. This alignment reinforces the consistency and reliability of the reported results across different studies and materials [50–53].

4 Conclusion

The CS: Fe550D and SS: SS550 reinforcements embedded in concrete under different chloride concentrations for corrosion durability and bond behaviour were studied. The following conclusions were drawn from the above study.

1. NCR test results showed that the weight loss and rate of corrosion of SS bars are significantly lower than the CS bars in different concentrations (0%, 3%, and 5%) of NaCl medium and it was found that CS bars have corroded 4–5 times than SS bars. From this it can be inferred that due to the presence of higher Chromium content, SS bars have shown great resistance towards corrosion than CS bars.
2. The results of the ACT revealed that the failure of CS bar specimens occurred at 4, 6, and 8 weeks in 0%, 3%, and 5% NaCl concentrations, respectively, while in the case of SS bar specimens, failure occurred at 15, 17, and 20 weeks in the same NaCl concentrations, respectively. This indicates that the time to failure of CS bars was approximately 3 times faster than SS bars. These findings clearly demonstrate that SS bars exhibit greater resistance to corrosion compared to conventional CS bars.
3. From the pull-out test results it can be understood that the bond strength of CS bars before corrosion was slightly higher than that of SS bars, whereas after corrosion the bond strength of CS bars was found to be 30% lower than that of SS bars.
4. The potentiometric titration analysis clearly indicated that the concentration of chloride ions in SS bars before corrosion was approximately twice as high as that in CS bars. This suggests that SS bars offer greater resistance to corrosion compared to CS bars.
5. The SEM analysis demonstrated that the chromium oxide film presents on the surface of the SS bars exhibited superior protective properties against stress corrosion cracking, voids, and crevices compared to the CS

bars in a chloride environment. This indicates that the presence of chromium in SS bars provides enhanced resistance to corrosion-related issues compared to CS bars.

Declarations

References

1. Green WK (2020) Steel reinforcement corrosion in concrete–an overview of some fundamentals. Corros Eng, Sci Technol 55(4):289–302
2. Richard B, The Concrete Society (1998) Guide on the use of stainless-steel reinforcement 2(1):155–165
3. Cramer SD, Covino BS Jr, Bullard SJ, Holcomb GR, Russell JH, Nelson FJ, Soltesz SM (2002) Corrosion prevention and remediation strategies for reinforced concrete coastal bridges. Cem Concr Compos 24(1):101–117
4. Apostolopoulos CA, Papadakis VG (2008) Consequences of steel corrosion on the ductility properties of reinforcement bar. Constr Build Mater 22(12):2316–2324
5. Nogueira CG, Leonel ED (2013) Probabilistic models applied to safety assessment of reinforced concrete structures subjected to chloride ingress. Eng Fail Anal 31:76–89
6. Mohammed TU, Otsuki N, Hamada H (2003) Corrosion of steel bars in cracked concrete under marine environment. J Mater Civ Eng 15(5):460–469
7. Quraishi MA, Nayak DK, Kumar R, Kumar V (2017) Corrosion of reinforced steel in concrete and its control: an overview. J Steel Struct Construct 3(1):1–6
8. Hansson CM, Poursaee A, Jaffer SJ (2012) Corrosion of reinforcing bars in concrete. Masterbuilder 15(3):106–124
9. Sika BT (2016) Refurbishment Protective Coatings for Concrete Sika Your Partner, vol 3, no 1. Sika, Hong Kong, China, pp 1–35
10. Zhao B (2007) Study on the Corrosion and Protection of the Coated Steel Rebar in Concrete. Xiamen University, Xiamen, China
11. Elnaggar EM, Elsokkary TM, Shohide MA, El-Sabbagh BA, Abdel-Gawwad HA (2019) Surface protection of concrete by new protective coating. Constr Build Mater 220:245–252
12. Diamanti MV, Brenna ANDREA, Bolzoni FABIO, Berra MARIO, Pastore T, Ormellese MARCO (2013) Effect of polymer modified cementitious coatings on water and chloride permeability in concrete. Constr Build Mater 49:720–728
13. Sohail MG, Salih M, Al Nuaimi N, Kahraman R (2019) Corrosion performance of mild steel and epoxy coated rebar in concrete

under simulated harsh environment. Int J Build Pathol Adapt 37(5):657–678

14. Sohail MG, Kahraman R, Alnuaimi NA, Gencturk B, Alnahhal W, Dawood M, Belarbi A (2020) Electrochemical behavior of mild and corrosion resistant concrete reinforcing steels. Constr Build Mater 232:117205

15. Cheng X, Xia J, Wu RJ, Jin WL, Pan CG (2022) Optimisation of sacrificial anode cathodic protection system in chloride-contaminated reinforced concrete structure. J Build Eng 45:103515

16. Wang F, Xu J, Xu Y, Jiang L, Ma G (2020) A comparative investigation on cathodic protections of three sacrificial anodes on chloride-contaminated reinforced concrete. Constr Build Mater 246:118476

17. NACE international (2016) International measures of prevention application and economics of corrosion technologies study. NACE International Houston, TX, USA

18. CIP 25- corrosion of steel in concrete (2020) Technical information prepared By NRMCA, vol 11, no 1, pp 1–2

19. Fontana MG, Greene ND (1967) Corrosion Engineering. McGraw-Hill, New York, vol 1, no 2, pp 1–391

20. Rowe J (ed) (2012) Advanced materials in automotive engineering. Elsevier, USA

21. Evans KJ, Rebak RB (2002) Corrosion science—a retrospective and current status in honor of robert p. Frankenthal PV 13:344–354

22. EN 10088–1 (2014) Stainless steels– Part 1: List of stainless steels, European Committee for Standardization, vol 1, pp 1–100

23. Outokumpu-Stainless (2009), The use of predictive models in specifying selective use of stainless-steel reinforcement

24. Nurnberger U (1996) Stainless steel in concrete: state of the art report. European Federation of Corrosion

25. Magnusson J (2000) Bond and anchorage of ribbed bars in high-strength concrete. Chalmers University of Technology

26. Lundgren K (2005) Bond between ribbed bars and concrete. Part 2: The effect of corrosion. Mag Concr Res 57(7):383–395

27. Allen JH, Felder AL, McDermott JF, Azizinamini A, Frosch RJ, Mitchell D, Matamoros AB (2003) Bond and development of straight reinforcing bars in tension. 408R(3):1–49

28. Lutz LA, Gergely P (1967) Mechanics of bond and slip of deformed bars in concrete. Journal 64(11):711–721

29. Alharbi YR, Galal M, Abadel AA, Kohail M (2021) Bond behavior between concrete and steel rebars for stressed elements. Ain Shams Eng J 12(2):1231–1239

30. Gunasekaran K, Kumar PS, Lakshmipathy M (2011) Mechanical and bond properties of coconut shell concrete. Constr Build Mater 25(1):92–98

31. Coccia S, Imperatore S, Rinaldi Z (2016) Influence of corrosion on the bond strength of steel rebars in concrete. Mater Struct 49:537–551

32. IS 16651 (2017) Strength Deformed Stainless Steel Bars and Wires for Concrete Reinforcement - Specification

33. IS 1786 (2008), High strength deformed steel bars and wires for reinforcement – specification

34. IS 10262 (2019), Concrete mix proportioning-Guidelines

35. American Society for Testing and Materials (ASTM) (2012) Standard guide for laboratory immersion corrosion testing of metals. ASTM Int 67:203–208

36. Malumbela G, Moyo P, Alexander M (2012) A step towards standardising accelerated corrosion tests on laboratory reinforced concrete specimens. J South African Inst Civil Eng= Joernaal van die Suid-Afrikaanse Instituut van Siviele Ingenieurswese 54(2):78–85

37. Irshidat MR (2021) Bond strength evaluation between steel rebars and carbon nanotubes modified concrete. Case Studies in Construct Materials 14:e00477

38. IS:3025 part-32 (1988), Methods of sampling and test (physical and chemical) for water and waste water.

39. Holder TB (1999) The determination of chloride threshold concentrations using different supplementary cementing materials in steel-reinforced concrete. University of Toronto

40. Andrade C, Alonso C (1996) Corrosion rate monitoring in the laboratory and on-site. Constr Build Mater 10(5):315–328

41. Andrade C, Alonso C (2001) On-site measurements of corrosion rate of reinforcements. Constr Build Mater 15(2–3):141–145

42. Bi M, Subramaniam K (2006) Corrosion of steel in cracked concrete: Experimental investigation. International corrosion conference series. National Association of Corrosion Engineers, Orlando, pp 557–562

43. Huttunen-Saarivirta E, Isotahdon E, Que Z, Lindgren M, Mardoukhi A, Jorcin JB, Mocnik P, Kosec T, El Ouazari Y, Mameng SH, Wegrelius L (2023) Pitting corrosion on highly alloyed stainless steels in dilute sulphuric acid containing sodium chloride. Electrochim Acta 457:142404

44. Martin-Perez, B. and Lounis, Z., 2003, May. Numerical modelling of service life of reinforced concrete structures. In: Life prediction and aging management of concrete structures, Proceedings of the 2 International RILEM workshop. (Eds) DJ Naus. PRO 29:71–79

45. FIB Bulletin (2001) Bond of reinforcement in concrete. Lausanne (CH), Switzerland, vol 1, no 2, pp 1–34

46. Rodriguez, J., Ortega, L. M., & Casal, J. (1994, June). Corrosion of reinforcing bars and service life of reinforced concrete structures: corrosion and bond deterioration. In: International conference on concrete across borders, Odense, Denmark. Taylor & Francis, Abingdon, UK. 2:315-326

47. Tondolo F (2015) Bond behaviour with reinforcement corrosion. Constr Build Mater 93:926–932

48. Villagrán-Zaccardi YA, Andrade C (2021) Chloride ingress rate and threshold content, as determined by the 'Integral'test method, in concrete with several w/c ratios in saturated and unsaturated conditions. Develop Built Environ 8:100062

49. Russo N, Gastaldi M, Schiavi L, Strini A, Lollini F (2023) Effects of cracks on chloride-induced corrosion initiation and propagation of carbon and stainless-steel rebar. Struct Concr 24(1):156–169

50. Song X, Y.qi Cai, C. Li (2020) Bond behavior between steel bars and carbon nanotube modified concrete. Constr Build Mater 255:119339

51. Rafi MM (2019) Study of bond properties of steel rebars with recycled aggregate concrete. Analyt Model, Strength Mater 51:166–174

52. Al-Shannag MJ, Charif A (2017) Bond behavior of steel bars embedded in concretes made with natural lightweight aggregates. J King Saud Univ - Eng Sci 29:365–372

53. Rafi MM (2018) Study of bond properties of steel rebars with recycled aggregate concrete. Experiment Test, Strength Mater 50:937–950